DOI: 10.1002/ejic.201000289

Vapour-Induced Amorphous–Crystalline Transformation of a Luminescent Platinum(II)–Diimine Complex

Atsushi Kobayashi,[a] Tsubasa Yonemura,[a] and Masako Kato*[a]

Keywords: Luminescence / Amorphous–crystalline transformation / Platinum / Vapochromism / Sensors

A novel luminescent platinum(II)–diimine complex, $Na_2[Pt(CN)_2(dcbpy)]\cdot nH_2O$ (H_2dcbpy = 4,4′-dicarboxy-2,2′-bipyridine, n = 2 or 5) was synthesized and investigated by using X-ray diffraction measurements and spectroscopy. Complex $Na_2[Pt(CN)_2(dcbpy)]\cdot 2H_2O$ was first obtained as a red amorphous solid (**1A**) that exhibits bright luminescence at 623 nm. After recrystallization, two crystalline forms, the dihydrate form, **1C**, and the pentahydrate form, $Na_2[Pt(CN)_2(dcbpy)]\cdot 5H_2O$ (**2**), were obtained and analyzed by the single-crystal X-ray diffraction method. Upon exposure of the amorphous form **1A** to hydrophilic vapours such as those of MeOH and acetone, **1A** irreversibly changed to a yellow crystalline solid **1C** that showed luminescence at 608 nm with a shoulder at 568 nm. This vapour-induced amorphous–crystalline transformation has never been observed either by exposing **1A** to hydrophobic vapours nor by increasing the temperature up to 410 K. IR spectroscopy revealed that the amorphous–crystalline transformation did not involve the adsorption of the vapour. This phenomenon of irreversible structural transformation accompanied by change of luminescence is possibly applicable to vapour *history* sensors.

Introduction

The design and synthesis of stable and reversible chemical sensors have received considerable attention in the past decade.[1] Vapochromic or vapoluminescent materials showing drastic colour or luminescence change upon exposure to vapours of volatile organic compounds (VOCs) are some of the most promising materials for sensing applications. Mann and co-workers reported on the vapochromic behaviour of the [Pt(aryl isocyanide)$_4$][Pd(CN)$_4$] complex and suggested that the intermolecular metallophilic interaction between d^8 metal ions plays a critical role in the chromic behaviour.[2] By taking advantage of the intermolecular metallophilic interaction mentioned in their report, much effort has been focused on developing new vapochromic materials that can be applied as chemical sensors.[3–10] One of the best-developed systems is a Pt^{II}–diimine system.[2–5] The vapochromic behaviour in this series usually originates from the structural change induced by adsorption of vapour molecules. The adsorption of vapour molecules changes the intermolecular metallophilic and/or π–π interactions, resulting in the perturbation of the transition energy in the visible region. For example, [Pt(bpy)(CN)$_2$] (bpy: 2,2′-bipyridine) is a simple vapochromic material showing bright luminescence from the metal-metal-to-ligand charge transfer (^{3}MMLCT) transition state and undergoing a reversible colour change upon exposure to water vapour.[5] This chromic behaviour is due to the water-vapour-induced structural transformation between nonhydrated [Pt(bpy)(CN)$_2$] and monohydrate [Pt(bpy)(CN)$_2$]·H$_2$O. The adsorption of water molecules changes the distance between the Pt ions, which mainly contributes to the energy of the HOMO, resulting in colour and luminescence changes. Similarly, vapochromic materials with metallophilic interaction among Au^I ions have also been reported.[6,7] Some of the Au^I complexes show not only vapochromism but also mechanochromism, which is the reversible colour change induced by the application of mechanical pressure.[7] Another approach is to incorporate well-established solvatochromic molecules into solid-state materials.[8] Incorporation of Tb^{3+} ions into the framework of a microporous solid permits shape- and size-selective sensing.[8b] Recently, some groups have reported that complexes of nonprecious metals can show vapochromic behaviour that originates from the vapour-induced transformation of the coordination environment of the metallic centre.[9] Most of these vapour-sensing abilities are basically derived from a *reversible* structural transformation induced by adsorption of vapour molecules. However, there are few examples showing a sensing ability based on an *irreversible* structural transformation. This type of transformation may be promising for vapour *history* sensors.

We also designed a vapochromic Pt^{II} complex, [Pt(CN)$_2$(H$_2$dcbpy)] (H$_2$dcbpy: 4,4′-dicarboxy-2,2′-bipyridine), and demonstrated that the flexible two-dimensional hydrogen

[a] Division of Chemistry, Faculty of Science, Hokkaido University,
North-10 West-8, Kita-ku, Sapporo, Hokkaido 060-0810, Japan
Fax: +81-11-706-3447
E-mail: mkato@sci.hokudai.ac.jp

Supporting information for this article is available on the WWW under http://dx.doi.org/10.1002/ejic.201000289.

bond networks formed between the cyano and carboxyl groups play an important role in the vapochromic behaviour.[10] Taking advantage of the coordination ability of the carboxyl and cyano groups of this complex, we focused our attention on the development of new sensing materials. In this work, we have synthesized a cation-substituted complex, $Na_2[Pt(CN)_2(dcbpy)]\cdot nH_2O$ (n = 2 and 5), and have found that the complex exhibits a vapour-induced amorphous–crystalline structural transformation accompanied by remarkable changes in colour and luminescence.

Results and Discussion

Vapour-Induced Amorphous–Crystalline Transformation

Complex $Na_2[Pt(CN)_2(dcbpy)]\cdot 2H_2O$ (**1**) was first obtained as a red amorphous solid (**1A**). Elemental analysis of **1A** clearly shows that the complex contains two water molecules per $Na_2[Pt(CN)_2(dcbpy)]$ unit. This red amorphous form is stable in dry air, but the colour gradually changes from red to yellow in humid air. In order to clarify the origin of this colour change, powder X-ray diffraction (PXRD) measurements were conducted on the amorphous red solid **1A** upon exposure to various vapours. Figure 1 shows the PXRD patterns of **1A** exposed to several kinds of vapours over a period of two weeks. Before exposure, the PXRD pattern was very broad, indicating that **1A** is an amorphous solid. After exposure to hydrophilic vapours such as MeOH and acetone, the pattern dramatically changed to one with many sharp peaks, which is characteristic of crystalline solids. Surprisingly, all the patterns obtained for the samples exposed to hydrophilic vapours were almost identical to each other and they essentially corresponded to those obtained for the crystal of the dihydrate form, **1C**. The transformation was almost completed within 1 d in a saturated MeOH vapour atmosphere (Figure S1). These results suggest that the amorphous solid **1A** changed to the crystalline phase **1C** (the structure of **1C** is discussed below) upon exposure to the hydrophilic vapours. It should be noted that the amorphous solid **1A** was never converted into the crystalline **1C** by raising the temperature up to 410 K (Figure S2). In the ^1H NMR spectra of the samples exposed to the vapour for two weeks, vapour molecules were hardly detected (Figure S3). In addition, IR spectra measured for samples exposed to acetone vapour suggested that the acetone vapour was not included in the solid (Figure S4). Thus, this structural transformation was triggered by exposure to the vapours, but the inclusion of vapour molecules into the solid did not occur. On the other hand, upon exposure to hydrophobic vapours such as Et_2O and $CHCl_3$, no change was observed, suggesting that the amorphous–crystalline transformation from **1A** to **1C** is probably related to the hydrophilic nature of the vapour. It should be emphasized that the amorphous solid **1A** has very poor solubility not only for hydrophobic solvents but also for hydrophilic ones, except for water. When exposed to water vapour, the PXRD pattern of **1A** was also converted to a pattern similar to that calculated for the crystal structure of **1C**, but other peaks that could not be indexed were also observed. Since the PXRD pattern of **1A** immersed in a small amount of water was almost identical to the pattern calculated from the structure of pentahydrate form **2** (Figure S5), the pattern may be due to other transformations, for example **1C** to **2**. The obtained crystalline solid of **1C** is thermally stable and **1C** could not be converted back to **1A** even under vacuum at a high temperature around 373 K. Thus, this vapour-induced amorphous–crystalline transformation is irreversible in the solid state. As described in the introduction, many vapochromic Pt^{II}–diimine complexes have been reported so far, and their vapochromic behaviour originates primarily from the adsorption of vapour molecules, resulting in the reversible colour change. In the case of the transformation from red amorphous **1A** to yellow crystalline **1C**, the structure was transformed irreversibly from **1A** to **1C** by exposure to hydrophilic vapour, but the adsorption of vapour did not occur except for water vapour. To the best of our knowledge, such ordering induced by vapour molecules has not been reported for the system based on the Pt^{II}–diimine complex so far.

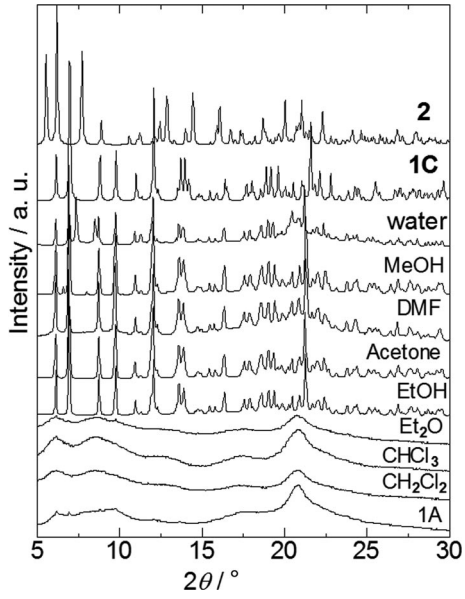

Figure 1. Changes in the powder X-ray diffraction pattern of **1A** upon exposure to several organic vapours. The two patterns labelled as **1C** and **2** are simulations based on the crystal structures of **1C** and **2** at 150 K. The exposure time for each vapour was two weeks at room temperature.

Crystal Structures

Dihydrate Form: $Na_2[Pt(CN)_2(dcbpy)]\cdot 2H_2O$

As discussed above, complex $Na_2[Pt(CN)_2(dcbpy)]\cdot 2H_2O$ (**1**) shows an interesting vapour-induced amorphous–crystalline transformation upon exposure to hydrophilic vapour. To determine the crystal structure of **1C** and **2**, we tried to obtain single crystals by using several recrystalli-

zation methods and succeeded for the pentahydrate form, $Na_2[Pt(CN)_2(dcbpy)]\cdot 5H_2O$ (**2**). From the single crystal of **2**, we successfully obtained a single crystal of **1C** by the single-crystal-to-single-crystal transformation (see Experimental Section). The transformation from **2** to **1C** was also confirmed by the thermogravimetric analysis of **2** by slow drying at room temperature (Figure S6). Although the quality of the single crystal became worse, it was still possible to determine the framework of the structure except for temperature factors. Figure 2a shows the crystal structure of the dihydrate form, **1C**. There are two chemically independent Na^+ ions and one $[Pt(CN)_2(dcbpy)]^{2-}$ anion in this crystal, indicating that the two carboxyl groups should be completely deprotonated. Although the molecular structure of the $[Pt(CN)_2(dcbpy)]^{2-}$ anion was similar to that of $[Pt(CN)_2(H_2dcbpy)]\cdot 4H_2O$,[10] the bond lengths around the carboxyl group in **1C** are significantly different from those in $[Pt(CN)_2(H_2dcbpy)]\cdot 4H_2O$. The four C–O bond lengths of the carboxyl groups are close to the typical value of the C–O bond length of carboxylate, indicating that the C–O bond order in **1C** is 1.5. In the IR spectra of **1C**, the stretching mode of the C–O bond was observed around 1650 cm^{-1} (see Figure S7). This result indicates that the two carboxyl groups were deprotonated and bound to Na ions. The two Na ions have a five-coordinate distorted square-pyramidal geometry. The Na1 ion is surrounded by one cyano nitrogen, three carboxyl oxygen atoms and one water molecule, while the Na2 ion is bound to two cyano nitrogen atoms and three carboxyl oxygen atoms. These two Na ions are μ-bridged by one carboxyl and one cyano group. Two independent water molecules are included in this crystal. One water molecule (labelled as O5) bridges two adjacent Na1 ions and another is weakly bound to the Na ion, with a distance of about 2.86(2) Å. As shown in Figure 2b, the bipyridine rings are stacked along the *a* axis. In this column, the intermolecular Pt–Pt distances [4.928(1) and 5.927(1) Å] are longer than twice the Van der Waals radius of the platinum atom (3.50 Å), indicating that the metallophilic interaction in this complex is negligibly weak. On the other hand, the relatively short distance between two adjacent bipyridine ligands (3.28 and 3.33 Å) suggests that the π–π interaction is effective in this column. This stacking manner of **1C** is quite different from that of the protonated complex $[Pt(CN)_2(H_2dcbpy)]\cdot 4H_2O$, whose crystal structure is supported by a two-dimensional hydrogen-bonding network and a metallophilic interaction between Pt ions,[10] implying that the structure of **1C** is mainly dominated by electrostatic potential rather than by hydrogen bonding or metallophilic interaction.

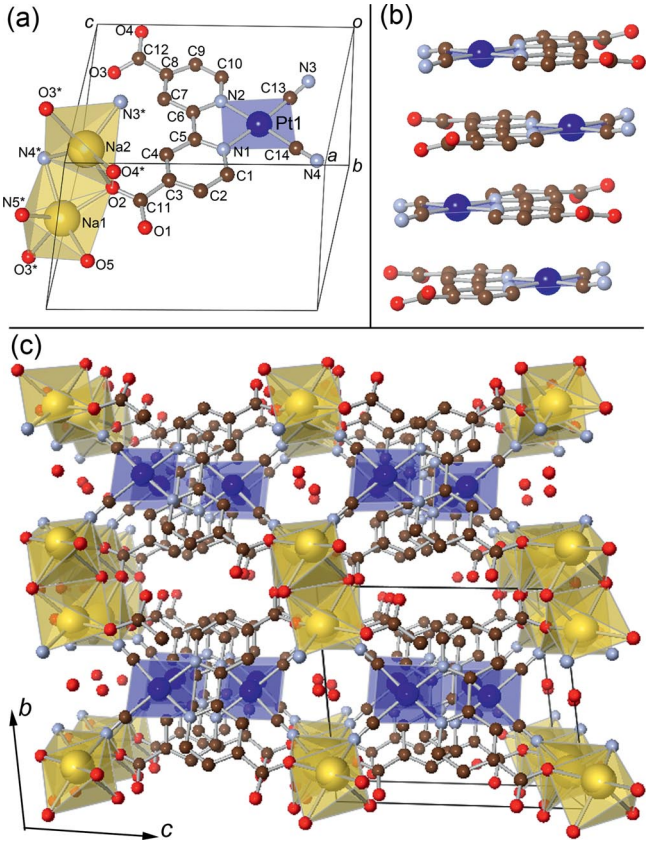

Figure 2. (a) Molecular structure of **1C**. (b) Stacked structure of $[Pt(CN)2(dcbpy)]^{2-}$ anions. (c) Perspective view of the crystal structure along the *a* axis of **1C** at 150 K. Blue planes and yellow polyhedrons show the coordination sphere of Pt and Na ions, respectively. Hydrogen atoms are omitted for clarity.

Pentahydrate Form: $Na_2[Pt(CN)_2(dcbpy)]\cdot 5H_2O$

As mentioned in the Experimental Section, the recrystallization of amorphous solid **1A** produced the pentahydrate form, $Na_2[Pt(CN)_2(dcbpy)]\cdot 5H_2O$ (**2**). Pentahydrate form **2** easily releases water of crystallization in air at room temperature. Thermogravimetric analysis indicates that **2** transformed into **1C** in dry N_2 atmosphere (Figure S6). To prevent the water of crystallization from being released during X-ray diffraction analysis of **2**, the single crystal was coated with paraffin oil and the diffraction measurement was conducted at low temperature (150 K). Figure 3 shows the crystal structure of pentahydrate form **2**. The observed bond lengths and angles around the $[Pt(CN)_2(dcbpy)]^{2-}$ unit were very similar to those of **1C**. The remarkable difference between **1C** and **2** is the coordination environment of the two Na ions. For complex **2**, two Na ions have octahedral coordination geometry. The Na1 ion is bound to two μ-bridged water molecules, one oxygen atom of carboxyl group and two water molecules, while the Na2 ion is bound to two cyano groups and two μ-bridged and two nonbridged water molecules. It was noteworthy that only one of the two carboxyl groups is directly bound to a Na ion in **2**. The $[Pt(CN)_2(dcbpy)]^{2-}$ unit is also stacked to form an almost uniform 1D column, which is similar to that in **1C**. The long intermolecular distances between two adjacent Pt ions [4.372(1) and 4.995(1) Å] are indicative of no Pt–Pt interaction. Judging from the distance between two adjacent bipyridine ligands (3.33 and 3.39 Å), the π–π interaction is moderately effective in **2** but weaker than that in **1C**.

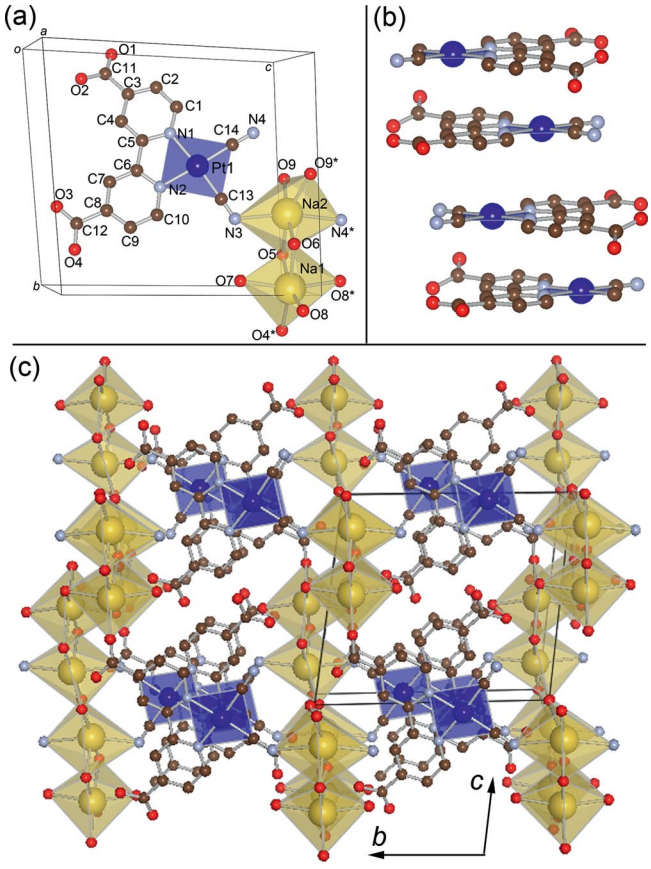

Figure 3. (a) Molecular structure of **2**. (b) Stacked structure of $[Pt(CN)2(dcbpy)]^{2-}$ anions. (c) Perspective view of crystal structure along the *a* axis at 150 K. Blue planes and yellow polyhedrons show the coordination sphere of Pt and Na ions, respectively. Hydrogen atoms are omitted for clarity.

Luminescence Properties

Since complex **1A** exhibited the irreversible amorphous–crystalline transformation induced by exposure to hydrophilic vapours, a change in luminescent properties after the transformation were expected. Figure 4 shows changes in the luminescence spectrum of **1A** upon exposure to MeOH vapour. Before exposure to MeOH, the amorphous solid **1A** showed a luminescence band at 623 nm, with a relatively high luminescence quantum yield (Φ_{em} = 0.27). The luminescence band shifted to a higher energy upon exposure to MeOH vapour. Simultaneously, a new emission band gradually appeared around 560 nm. As described above, red amorphous solid **1A** changed gradually to yellow crystalline solid **1C** (Figure 5). Thus, this change in the luminescence spectrum may be attributed to this transformation. Actually, the crystalline solid of **1C** exhibits an emission band at 608 nm, with a shoulder around 562 nm (Φ_{em} = 0.42), which is almost the same as that of the spectrum of **1A** exposed to MeOH vapour. Slight disagreement of the emission spectra of **1C** and **1A** under exposure to MeOH vapour may be due to the difference of the surface state of the solid. It is well known that the emission energy of the solid can be affected by the surface state. Under exposure to MeOH vapour, surface adsorption may contribute to the shift of the emission energy. It is well known that the emission energy of the platinum(II)–diimine complex tends to depend on both the degree of metallophilic interaction between Pt ions and the π–π interaction between diimine ligands.[11] Considering the crystal structure of **1C**, this change in the emission spectrum is due to the modification of these intermolecular interactions. We believe that this vapour-induced luminescence colour change from red to yellow is a unique phenomenon that could be applicable to vapour *history* sensors.

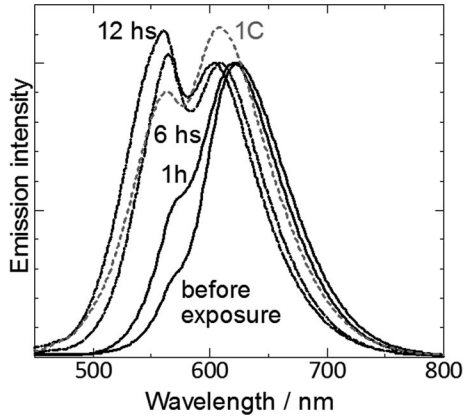

Figure 4. Exposure-time-dependence of the luminescence spectrum of **1A** under MeOH vapour. The grey dotted line shows the luminescence spectrum of **1C**; $\lambda_{ex.}$ = 400 nm.

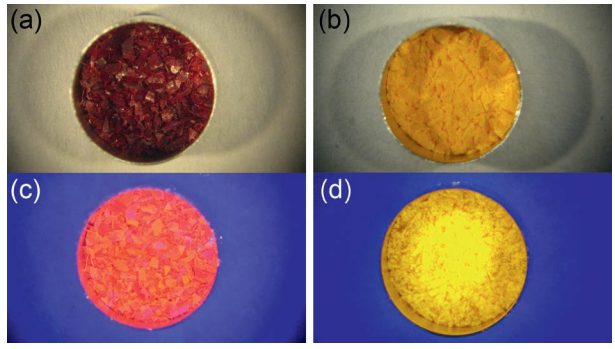

Figure 5. Bright-field images of **1A** (a) and **1C** (b). Luminescence images of **1A** (c) and **1C** (d). The sample of **1C** was obtained from the exposure of **1A** to MeOH vapour.

Conclusions

We synthesized and investigated a novel luminescent Pt^{II}–diimine complex, $Na_2[Pt(CN)_2(dcbpy)]\cdot nH_2O$ (*n*: 2 or 5). The complex was synthesized as an amorphous dihydrate solid, **1A**, which exhibits bright luminescence at 623 nm. Amorphous solid **1A** is stable in dry air and at high temperatures up to 410 K. An irreversible amorphous–crystalline transformation from **1A** to dihydrate crystalline **1C** was not triggered by hydrophobic vapours but by hydrophilic vapours such as MeOH, acetone, dmf, and so on. After the transformation, the colour changed from red to

yellow, and the luminescence band shifted to 600 nm with a new peak at 560 nm; this corresponds to the spectrum of **1C**. Most vapochromism observed for a series of Pt^{II}–diimine complexes is derived from the structural transformation induced by the adsorption of the vapour. However, it is interesting that the vapours could not be adsorbed by the amorphous solid **1A**. Thus, this transformation may be derived from a new type of structural modification induced by vapours without adsorption of the vapours. This irreversible colour change is a promising phenomenon applicable to new types of vapour *history* sensors.

Experimental Section

Syntheses: Starting material $[Pt(CN)_2(H_2dcbpy)]\cdot 2H_2O$ was synthesized according to the published method.[10]

Amorphous Solid $Na_2[Pt(CN)_2(dcbpy)]\cdot 2H_2O$ (1A): The purple powder of $[Pt(CN)_2(H_2dcbpy)]\cdot 2H_2O$ (200 mg, 0.379 mmol) was suspended in MeOH (5 mL). To this reddish-pink suspension was added a 28% MeOH solution of sodium methoxide (100 μL, 1.61 mmol). The colour of the suspension turned orange immediately. The product was collected by filtration, washed with MeOH and dried in vacuo to yield 125.4 mg {57.9% based on $[Pt(CN)_2(H_2dcbpy)]\cdot 2H_2O$} of $Na_2[Pt(CN)_2(dcbpy)]\cdot 2H_2O$ (**1A**) as a red amorphous powder. This synthesis of **1A** was conducted in air before drying. $C_{14}H_6N_4Na_2O_4Pt\cdot 2H_2O$ (571.32): calcd. C 29.43, H 1.76, N 9.81; found C 29.14, H 2.06, N 9.64. Since this amorphous solid gradually changed to the dihydrated crystalline **1C** in humid air, the solid was stored in a dried Ar atmosphere.

Crystalline Solid Pentahydrated Complex $Na_2[Pt(CN)_2(dcbpy)]\cdot 5H_2O$ (2): The red powder of **1A** (50 mg) was dissolved in water (0.6 mL). To this yellow solution was added MeOH (0.8 mL). Diffusion of ethyl ether into this water–MeOH mixed solution gave the pale yellow crystalline solid of **2** (yield: 8.5 mg, 15.5%). $C_{14}H_6N_4Na_2O_4Pt\cdot 5H_2O$ (625.36): calcd. C 26.89, H 2.58, N 8.96; found C 26.96, H 2.64, N 8.93.

Crystalline Solid Dihydrated Complex $Na_2[Pt(CN)_2(dcbpy)]\cdot 2H_2O$ (1C): The crystalline solid of dihydrated complex **1C** has not been obtained from the recrystallization of **1A**. The crystalline solid of **1C** was obtained by slow drying of pentahydrate complex **2**. $C_{14}H_6N_4Na_2O_4Pt\cdot 2H_2O$ (571.32): calcd. C 29.43, H 1.76, N 9.81; found C 29.50, H 1.83, N 9.75.

Single-Crystal X-ray Diffraction Measurement: A single crystal was mounted on a glass fibre with silicon grease. Since the single crystal of **2** was not stable in air at room temperature, the crystal was coated with paraffin oil and quickly cooled down to 150 K. All measurements were made with a Rigaku AFC-7R diffractometer with a Mercury CCD area detector, graphite monochromated Mo-K_a radiation (λ = 0.71069 Å) and a rotating anode generator. The data were collected at a temperature of 150 ± 1 K to a maximum 2θ value of 59.2°. The Pt atom was refined anisotropically and the other atoms were refined isotropically for **1C**. The non-hydrogen atoms were refined anisotropically and the hydrogen atoms were refined isotropically for **2**. The structures were solved by direct methods (SIR92)[12] and expanded by using Fourier techniques (DIRDIF99).[13] All calculations were performed with the CrystalStructure crystallographic software package,[14] except for refinement, which was performed by using SHELXL-97.[15] A summary of the crystallographic data for dihydrated form **1C** and pentahydrated form **2** is given in Table 1. CCDC-769439 and -769440 contain the supplementary crystallographic data for this paper. These data can be obtained free of charge from The Cambridge Crystallographic Data Centre via www.ccdc.cam.ac.uk/data_request/cif.

Table 1. Crystallographic data for **1C** and **2**.

Complex	**1C**	**2**
Chemical formula	$C_{14}H_6N_4Na_2O_4Pt\cdot 2H_2O$	$C_{14}H_6N_4Na_2O_4Pt\cdot 5H_2O$
Temperature /K	150	150
Crystal system	triclinic	tricilinic
Space group	$P\bar{1}$	$P\bar{1}$
a /Å	7.137(4)	6.969(2)
b /Å	9.981(5)	11.618(3)
c /Å	11.292(6)	12.600(4)
α /°	83.25(2)	80.152(9)
β /°	83.46(2)	82.203(9)
γ /°	82.73(2)	74.394(8)
V /Å^3	788.3(7)	963.7(5)
Z	2	2
$D_{calcd.}$ /Mg m^{-3}	2.390	2.120
Collected reflections	5160	7895
Unique reflections	2718	4363
No. of parameters	245	272
R	0.0473	0.0338
R_w[a]	0.0745	0.0902
Goodness-of-fit	1.163	1.066

[a] $R_W = [\Sigma(w(F_o^2 - F_c^2)^2)/\Sigma w(F_o^2)^2]^{1/2}$.

Powder X-ray Diffraction: Powder X-ray diffraction patterns [λ = 1.200(1) Å] of the samples were measured at the BL-8B beamline in a photon factory at KEK, Japan.

Luminescence Properties: The luminescence spectra of the samples were measured by using a JASCO FR-6600 spectrofluorometer at room temperature. About 1 mg of the sample was placed in a glass capillary of 0.5 mm in diameter. Slit widths of excitation and emission light were 5 and 6 nm, respectively. Luminescence quantum efficiency was recorded with a HAMAMATSU C9920-02 absolute photoluminescence quantum yield measurement system.

Thermogravimetric Analysis: Thermogravimetry and differential thermal analysis were performed by using a Rigaku ThermoEvo TG8120 analyzer.

Supporting Information (see footnote on the first page of this article): Exposure time and temperature dependences of PXRD patterns of **1A**, IR spectra, ^{1}H NMR spectra and thermogravimetric analysis are presented.

Acknowledgments

This work is supported by a Grant-in-Aid for Scientific Research, Photochromism (No.471), Young Scientists (B) (19750050) and the Global COE Program (Project No. B01: Catalysis as the Basis for Innovation in Materials Science) from the Ministry of Education, Culture, Sports, Science and Technology, Japan.

[1] M. H. Keefe, K. D. Benkstein, J. T. Hupp, *Coord. Chem. Rev.* **2000**, *205*, 201–228.

[2] a) C. L. Exstrom, J. R. Sowa, C. A. Daws, D. Janzen, K. R. Mann, *Chem. Mater.* **1995**, *7*, 15–17; b) C. A. Daws, C. L. Exstrom, J. R. Sowa, K. R. Mann, *Chem. Mater.* **1997**, *9*, 363–368; c) Y. Kunugi, L. L. Miller, K. R. Mann, M. K. Pomije, *Chem. Mater.* **1998**, *10*, 1487–1489; d) C. L. Exstrom, M. K. Pomije, K. R. Mann, *Chem. Mater.* **1998**, *10*, 942–945; e) Y. Kunugi, K. R. Mann, L. L. Miller, C. L. Exstrom, *J. Am. Chem. Soc.* **1998**, *120*, 589–590; f) S. M. Drew, D. E. Janzen,

C. E. Buss, D. I. MacEwan, K. M. Dublin, K. R. Mann, *J. Am. Chem. Soc.* **2001**, *123*, 8414–8415; g) C. E. Buss, K. R. Mann, *J. Am. Chem. Soc.* **2002**, *124*, 1031–1039.

[3] a) L. J. Grove, A. G. Oliver, J. A. Krause, W. B. Connick, *Inorg. Chem.* **2008**, *47*, 1408–1410; b) W. Lu, M. C. W. Chan, N. Zhu, C.-M. Che, Z. He, K.-Y. Wong, *Chem. Eur. J.* **2003**, *9*, 6155–6166; c) T. J. Wadas, Q.-M. Wang, Y.-J. Kim, C. Flaschenreim, T. N. Blanton, R. Eisenberg, *J. Am. Chem. Soc.* **2004**, *126*, 16841–16849; d) S. C. F. Kui, S. S.-Y. Chui, C.-M. Che, N. Zhu, *J. Am. Chem. Soc.* **2006**, *128*, 8297–8309; e) L. L. Grove, J. M. Rennekamp, H. Jude, W. B. Connick, *J. Am. Chem. Soc.* **2004**, *126*, 1594–1595; f) N. Albrecht, M. Lutz, A. L. Spek, G. v. Koten, *Nature* **2000**, *406*, 970–974; g) J. Fornies, S. Fuertes, J. A. Lopez, A. Martin, V. Sicilia, *Inorg. Chem.* **2008**, *47*, 7166–7176; h) M. L. Muro, C. A. Daws, F. N. Castellano, *Chem. Commun.* **2008**, 6134–6136; i) J. Ni, Y.-H. Wu, X. Zhang, B. Li, L.-Y. Zhang, Z.-N. Chen, *Inorg. Chem.* **2009**, *48*, 10202–10210; J. S. Field, C. D. Grimmer, O. Q. Munro, B. P. Waldron, *Dalton Trans.* **2010**, *39*, 1558–1567.

[4] a) M. Kato, A. Omura, A. Toshikawa, S. Kishi, Y. Sugimoto, *Angew. Chem. Int. Ed.* **2002**, *41*, 3183–3185; b) M. Kato, *Bull. Chem. Soc. Jpn.* **2007**, *80*, 287–294; c) A. Kobayashi, Y. Fukuzawa, S. Noro, T. Nakamura, M. Kato, *Chem. Lett.* **2009**, *38*, 998–999; d) A. Kobayashi, H. Hara, S. Noro, M. Kato, *Dalton Trans.* **2010**, in press.

[5] a) M. Kato, C. Kosuge, K. Morii, J. S. Ahn, H. Kitagawa, T. Mitani, M. Matsushita, T. Kato, S. Yano, M. Kimura, *Inorg. Chem.* **1999**, *38*, 1638–1641; b) S. Kishi, M. Kato, *Mol. Cryst. Liq. Cryst.* **2002**, *379*, 303–308.

[6] a) J. C. Vickery, M. M. Olmstead, E. Y. Fung, A. L. Balch, *Angew. Chem. Int. Ed. Engl.* **1997**, *36*, 1179–1181; b) M. A. Mansour, W. B. Connick, R. J. Lachicotte, H. J. Gysling, R. Eisenberg, *J. Am. Chem. Soc.* **1998**, *120*, 1329–1330; c) A. Hayashi, M. M. Olmstead, S. Attar, A. L. Balch, *J. Am. Chem. Soc.* **2002**, *124*, 5791–5795; d) E. J. Fernandez, J. M. Lopez-de-Luzuriaga, M. Monge, M. Montiel, M. E. Olmos, J. Perez, A. Laguna, F. Mendizabal, A. A. Mohamed, J. P. Fackler Jr., *Inorg. Chem.* **2004**, *43*, 3573–3581.

[7] H. Ito, T. Saito, N. Oshima, N. Kitamura, S. Ishizaka, Y. Hinatsu, M. Wakeshima, M. Kato, K. Tsuge, M. Sawamura, *J. Am. Chem. Soc.* **2008**, *130*, 10044–10045.

[8] a) J. L. Meinershagen, T. Bein, *J. Am. Chem. Soc.* **1999**, *121*, 448–449; b) T. M. Reineke, M. Eddaoudi, M. Fehr, D. Kelley, O. M. Yaghi, *J. Am. Chem. Soc.* **1999**, *121*, 1651–1657.

[9] a) E. Cariati, X. Bu, P. C. Ford, *Chem. Mater.* **2000**, *12*, 3385–3391; b) N. Baho, D. Zargarian, *Inorg. Chem.* **2007**, *46*, 299–308; c) L. G. Beauvais, M. P. Shores, J. R. Long, *J. Am. Chem. Soc.* **2000**, *122*, 2763–2772; d) E. J. Fernandez, J. M. Lopez-de-Luzuriaga, M. Monge, M. E. Olmos, R. C. Puelles, A. Laguna, A. A. Mohamed, J. P. Fackler Jr., *Inorg. Chem.* **2008**, *47*, 8069–8076; e) A. Bencini, M. Casarin, D. Forrer, L. Franco, F. Garau, N. Masciocchi, L. Pandolfo, C. Pettinari, M. Ruzzi, A. Vittadini, *Inorg. Chem.* **2009**, *48*, 4044–4051; f) Z. Liu, Z. Bian, J. Bian, Z. Li, D. Nie, C. Huang, *Inorg. Chem.* **2008**, *47*, 8025–8030.

[10] M. Kato, S. Kishi, Y. Wakamatsu, Y. Sugi, Y. Osamura, T. Koshiyama, M. Hasegawa, *Chem. Lett.* **2005**, *34*, 1368–1369.

[11] a) J. A. Bailey, M. G. Hill, R. E. Marsh, V. M. Miskowski, W. P. Schaefer, H. B. Gray, *Inorg. Chem.* **1995**, *34*, 4591–4599; b) A. Y.-Y. Tam, K. M.-C. Wong, G. Wang, V. W.-W. Yam, *Chem. Commun.* **2007**, 2028–2030; c) V. W.-W. Yam, K. M.-C. Wong, N. Zhu, *J. Am. Chem. Soc.* **2002**, *124*, 6506–6506; d) V. W.-W. Yam, K. H.-Y. Chan, K. M.-C. Wong, N. Zhu, *Chem. Eur. J.* **2005**, *11*, 4535–4543; e) S.-Y. Lai, H.-W. Lam, W. Lu, K.-K. Cheung, C.-M. Che, *Organometallics* **2002**, *21*, 226–234.

[12] SIR-92; A. Altomare, G. Cascarano, C. Giacovazzo, A. Guagliardi, M. Burla, G. Polidori, M. Camalli, *J. Appl. Crystallogr.* **1994**, *27*,435.

[13] P. T. Beurskens, G. Admiraal, G. Beurskens, W. P. Bosman, R. deGelder, R. Israel, J. M. M. Smits, *DIRDIF99*, Crystallography Laboratory at University of Nijmegen: Nijmegen, The Netherlands, **1999**.

[14] *CrystalStructure 3.8*, Crystal Structure Analysis Package, Rigaku and Rigaku/MSC, 9009 New Trails Dr. The Woodlands TX 77381 USA, **2000**–**2006**.

[15] *SHELXL-97*: G. M. Sheldrick, *Acta Crystallogr., Sect. A* **2008**, *64*, 112.

Received: March 14, 2010
Published Online: April 28, 2010

